Teoretyczny opis wzbudzonych jąder atomowych:
Powracajace nadprzewodnictwo w stanach wysokospinowych
Izentropowe ścieżki do rozszczepienia jąder złożonych

Witold Nazarewicz

Wydział Fizyki UW, Grudzień 2009

When a metal is cooled below its superconducting transition temperature T_c in the presence of an external magnetic field, the magnetic flux inside vanishes. For type I superconductors, magnetic flux is expelled below a critical field H_c, while at $H=H_c$, a sharp transition to a normal conductor takes place. In type II superconductors, this transition is gradual, and it is characterized by two critical temperatures, T_{c1} and T_{c2}. For $T_{c1} < T < T_{c2}$ the system exists in the vortex (mixed) state in which the normal and superconducting phases *coexist*.

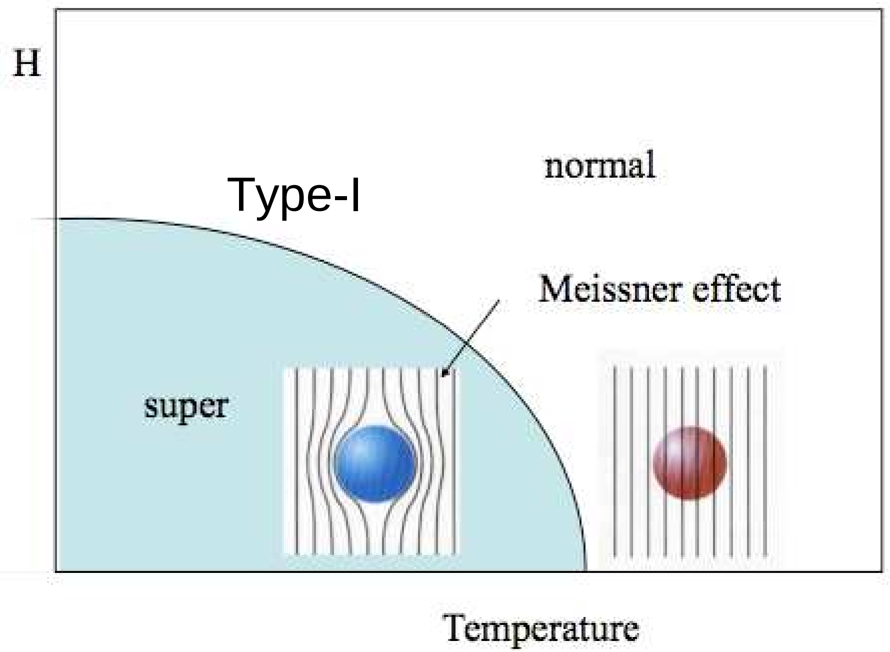

Recently, there has been increased interest in properties of polarized (asymmetric) Fermi systems with unusual pairing configurations. This includes the existence of superconductivity in a ferromagnetically ordered phase and an interplay between pairing, spin polarization, and temperature in condensates having an unequal number of spin-up and spin-down fermions.

What about nuclei?

Polarization -> Angular momentum
Vortices -> Broken pairs

- Mottelson-Valatin effect (1960)
- Backbending and pair decoupling (1972)
- Nuclei are Type-II superconductors (Birbrair 1971)

$$H \longrightarrow \omega$$

$$M \longrightarrow J$$

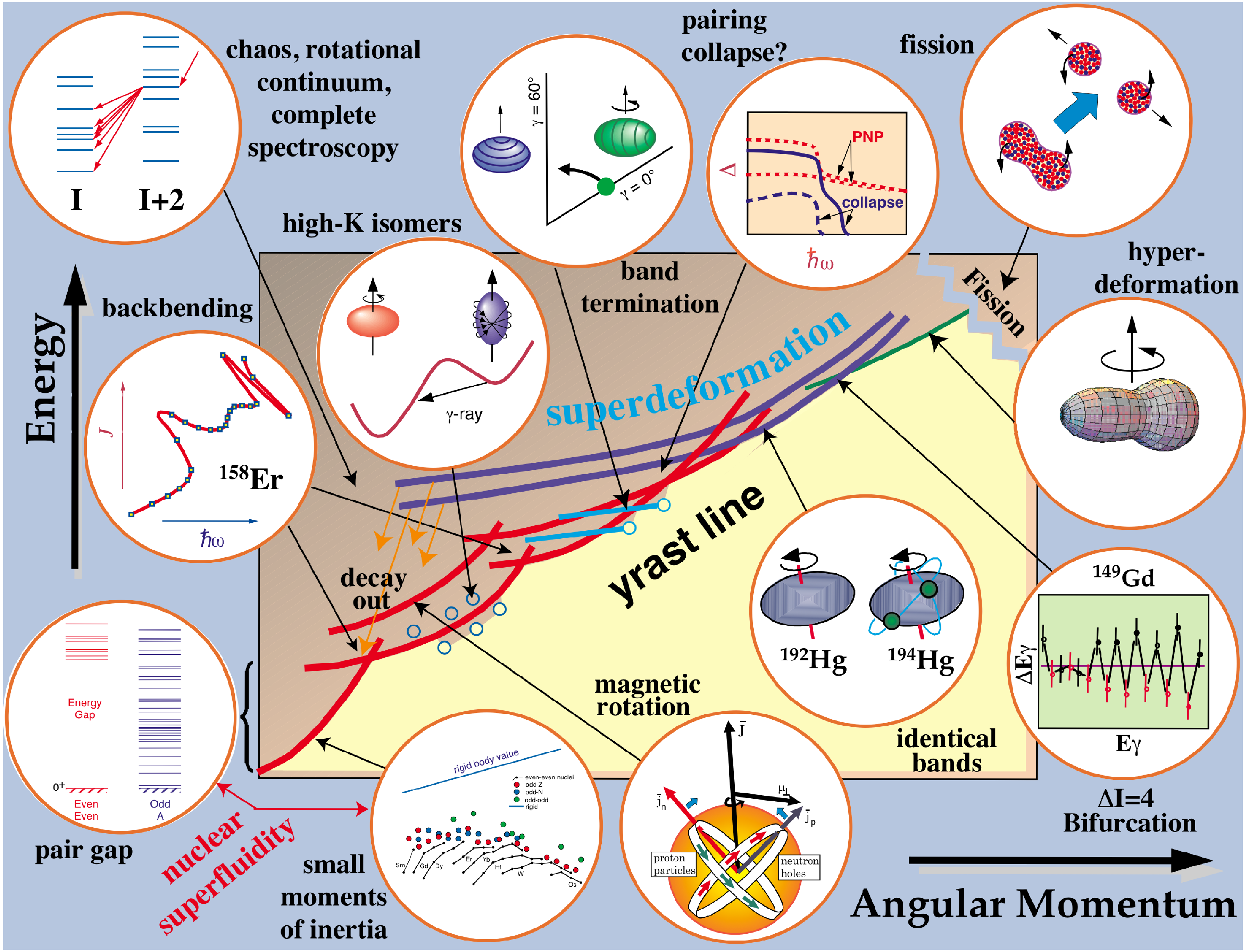chaos, rotational continuum, complete spectroscopy
I
I+2
γ = 60°
γ = 0°
pairing collapse?
PNP
Δ
collapse
ħω
fission
high-K isomers
γ-ray
band termination
hyper-deformation
Fission
Energy
backbending
J
^{158}Er
ħω
superdeformation
decay out
yrast line
^{192}Hg
^{194}Hg
^{149}Gd
ΔEγ
Eγ
Energy Gap
0+
Even Even
Odd A
pair gap
nuclear superfluidity
rigid body value
even-even nuclei
odd-Z
odd-N
odd-odd
rigid
Sm
Gd
Dy
Er
Yb
Hf
W
Os
small moments of inertia
magnetic rotation
J̄
μ⊥
j̄n
j̄p
proton particles
neutron holes
identical bands
ΔI=4 Bifurcation
Angular Momentum

The majority of investigations have been restricted to rotating cold nuclei or to non-rotating heated nuclei, thus exploring only limits of the (ω, T) phase diagram

Meissner effect and reentrance phenomenon in heated rotating nuclei

D.J. Dean, K. Langanke, H.A. Nam, and WN

submitted, arXiv:0901.0560

Previous work:

Thermal properties of N=40 isotopes K. Langanke, D.J. Dean, WN
Nucl. Phys. A 757 (2005) 360

Temperature-induced superconductor-to-normal and deformed-to-spherical phase transition in N=40 medium-mass isotones:

- ^{68}Ni - spherical, weakly-paired
- ^{70}Zn - spherical, superfluid
- ^{72}Ge - deformed, superfluid
- ^{80}Zr - deformed, weakly-paired

The deformed-to-spherical transition is fairly gradual, and it does not produce a peak in the specific heat.

The calculations nicely differentiate between two limits of pairing correlations. For superfluid systems (static pairing), the superfluid-to-normal transition manifests itself as a pronounced peak in the specific heat around T=0.6-0.7 MeV. For nuclei with weak (dynamic) pairing, C_V increases in a smooth way. Here, the notion of a phase transition cannot be applied.

The Model

Complete *fp-gds* shell-model space (the Shottky peak moved to T>2 MeV)
Shell Model Monte Carlo Method (SMMC)

$$\langle A \rangle = \frac{\mathrm{Tr}_{\mathcal{N}}(A e^{-\beta H})}{\mathrm{Tr}_{\mathcal{N}} e^{-\beta H}}$$

Nuclear observables described as thermal averages

$$Z(\beta) = \mathrm{Tr}_{\mathcal{N}} e^{-\beta\left(\sum_\alpha \varepsilon_\alpha \mathcal{O}_\alpha + \sum_\alpha V_\alpha \mathcal{O}_\alpha^2\right)}$$

Single-Particle Hamiltonian (^{56}Ni) + pairing+quadrupole term

$$H = \sum_{jmt_z} \epsilon(j) a^\dagger_{jmt_z} a_{jmt_z} - \frac{G}{4} \sum_{\alpha,\alpha',t_z} P^\dagger_{JT=01,t_z}(\alpha) P_{JT=01,t_z}(\alpha') - \chi \sum_\mu (-1)^\mu Q_{2\mu} Q_{2-\mu}$$

4096 statistical samples

Fock space: (0f1p – 0g1d2s)

^{72}Ge: 12 valence protons, 20 valence neutrons

$$\hat{H}^\omega = \hat{H} - \omega \hat{J}_z$$

Includes time-odd physics

Highly-asymmetric pattern:
interplay between alignment and pairing

12 valence protons, 20 valence neutrons
in practice: 4 valence protons, 12 valence neutrons

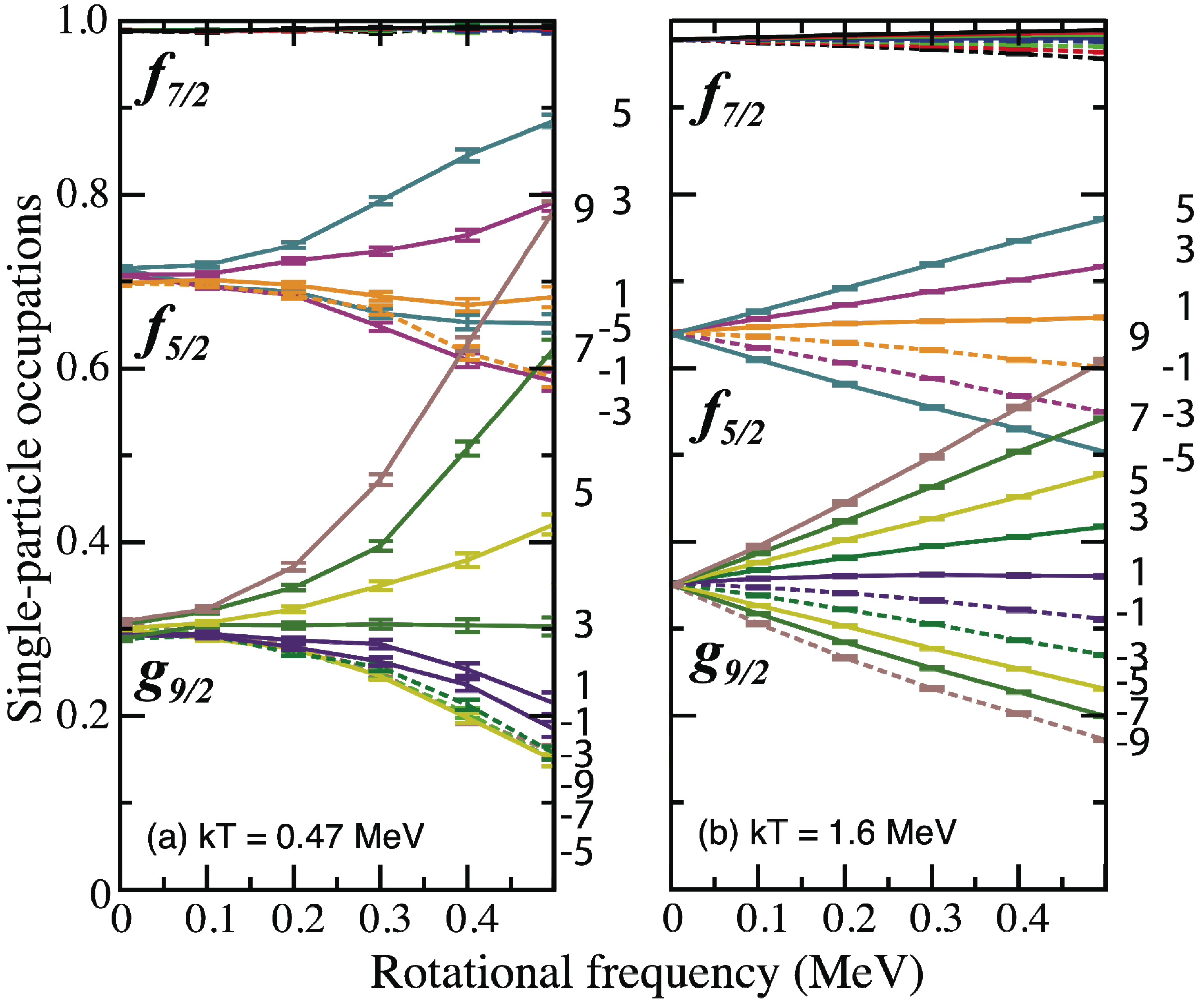

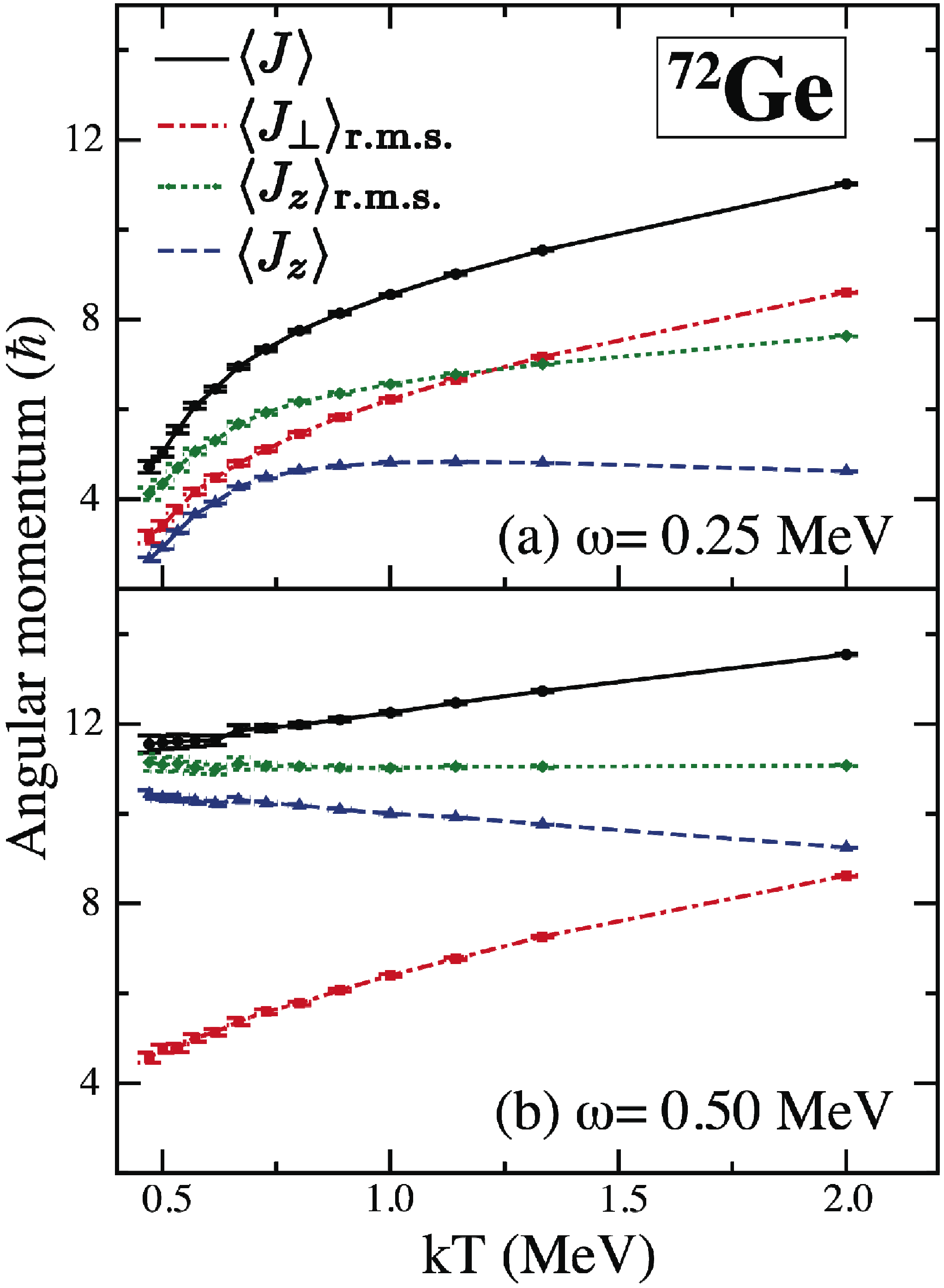

One broken $g_{9/2}$ neutron pair

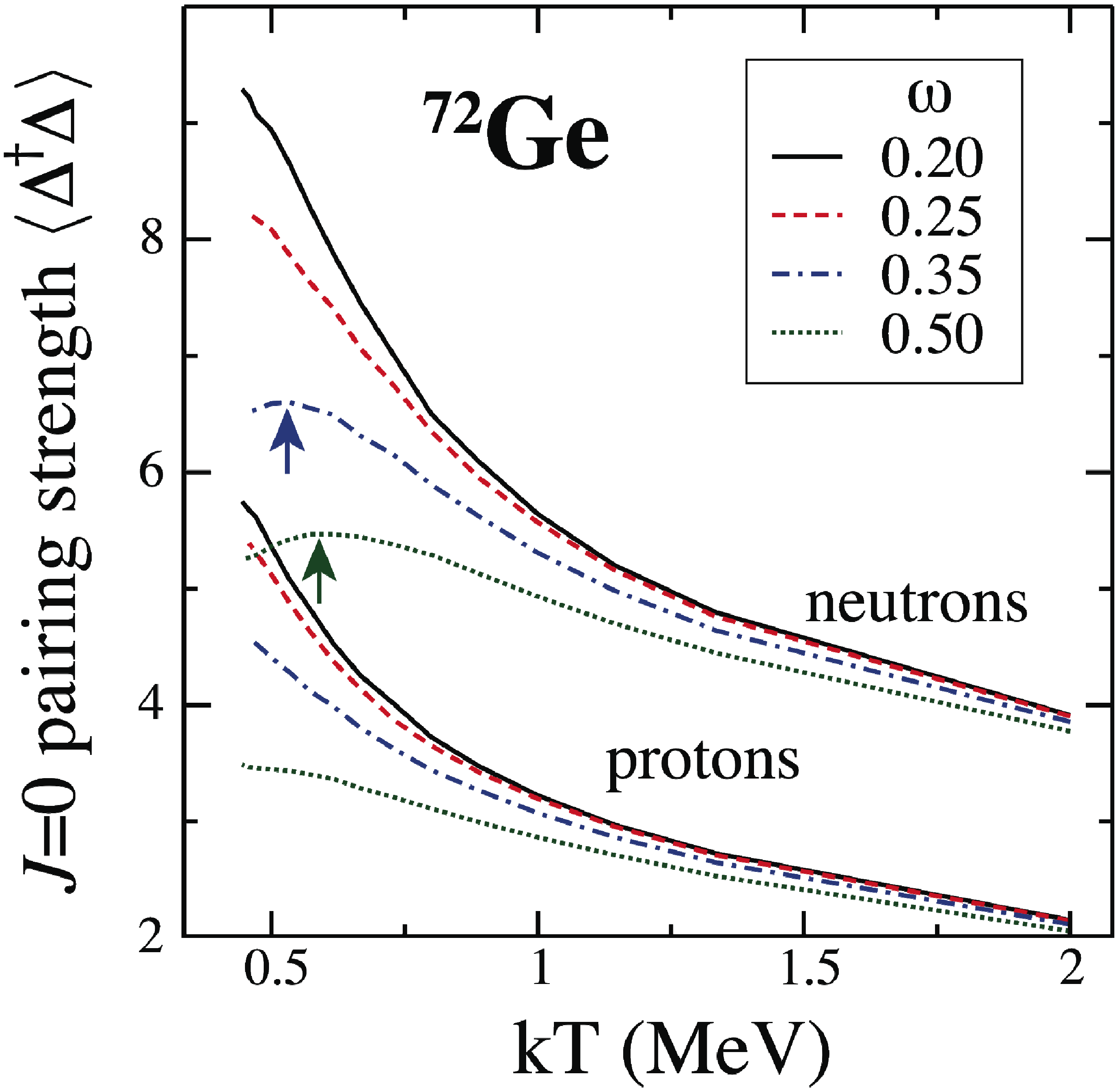

^{72}Ge
ω
0.20
0.25
0.35
0.50
neutrons
protons
J=0 pairing strength $\langle \Delta^\dagger \Delta \rangle$
kT (MeV)
2
4
6
8
0.5
1
1.5
2

Reentrant superconductivity

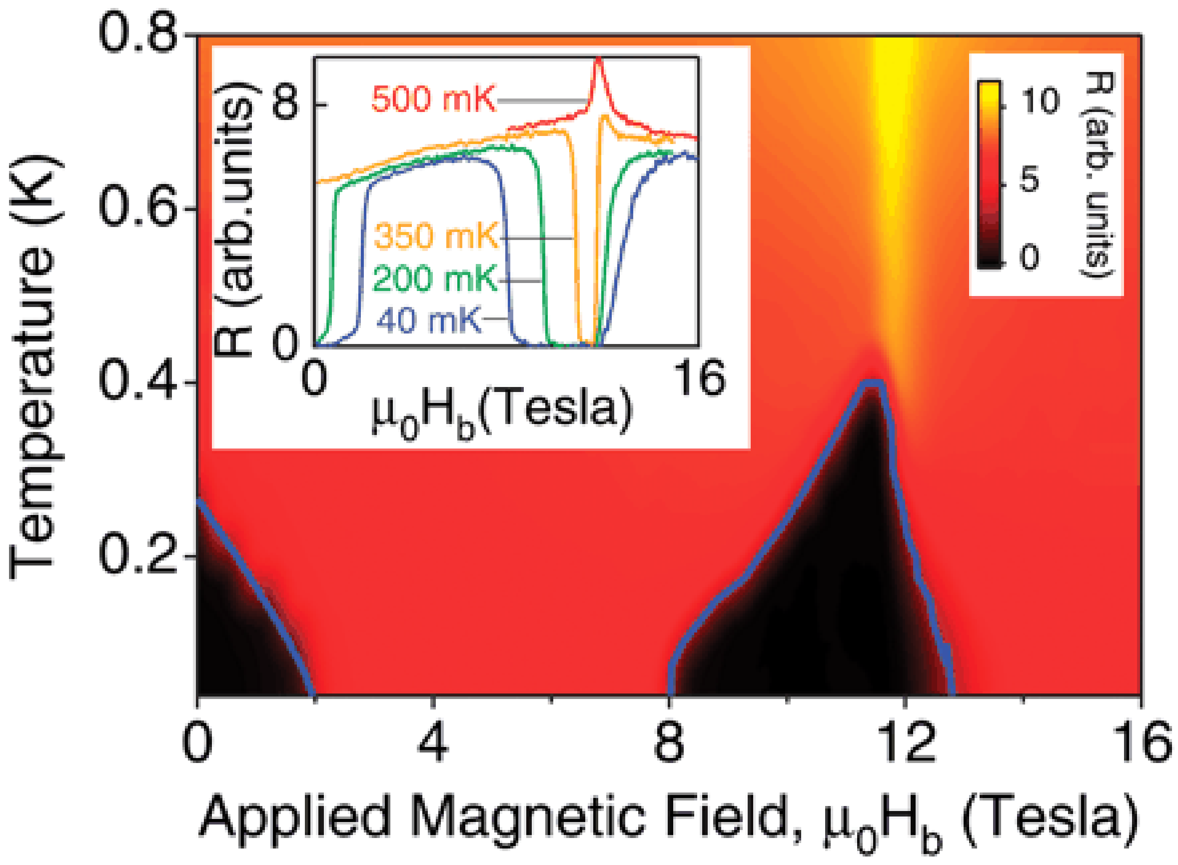

Magnetic Field-Induced Superconductivity in the Ferromagnet URhGe
F. Lévy, *et al.*
Science 309, 1343 (2005)

“We report that a second pocket of super- conductivity occurs at low temperature for a range of fields enveloping this magnetic transition, well above the field of 2T at which superconductivity is first destroyed.”

The reentrance (or partial order) phenomenon manifests itself in successive phase transitions

Reentrant superconductivity

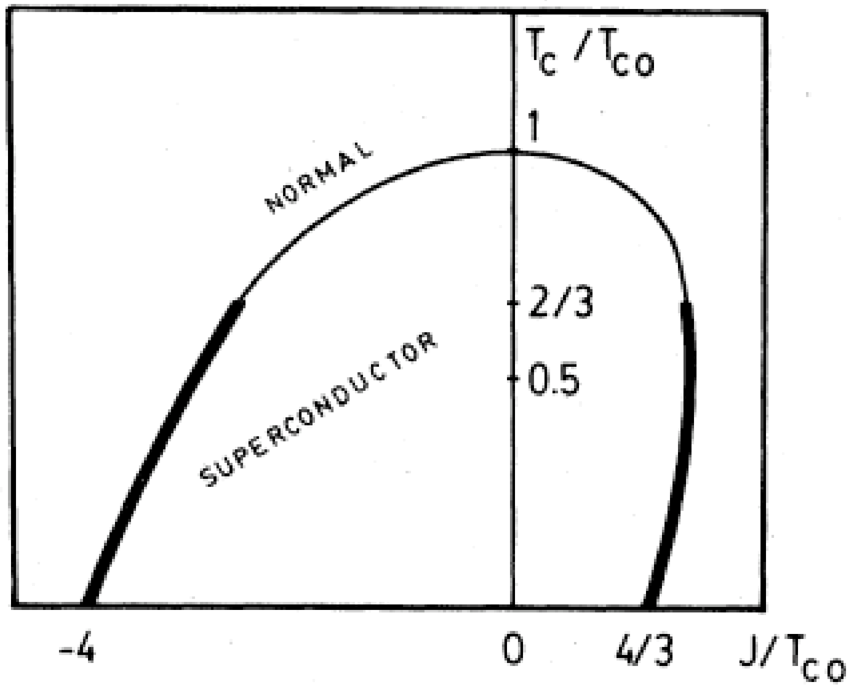

FIG. 2. Phase diagram obtained with the zero-bandwidth limit of the MHZ (Ref. 14) model [including both ferromagnetic ($J < 0$) and antiferromagnetic ($J < 0$) values of the exchange constant]. In the last case the phenomenon of reentrance is observed. —— second-order phase transition, ▬ first-order phase transition.

Allub, Wiecko, Alascio
Phys. Rev. B 23, 1122 (1981)
Ce impurities in superconductors

- S. Robaszkiewicz, R. Micnas, and J. Ranninger, Phys. Rev. B 36, 180 (1987).
- N.A. Fortune et al., Phys. Rev. Lett. 64, 2054 (1990).
- H.T. Diep, M. Debauche, and H. Giacomini, Phys. Rev. B 43, 8759 (1991).
- F.M. Araujo-Moreira, W. Maluf, and S. Sergeenkov, Eur. Phys. J. B 44, 33 (2005).

The reentrance (or partial order) phenomenon manifests itself in successive phase transitions

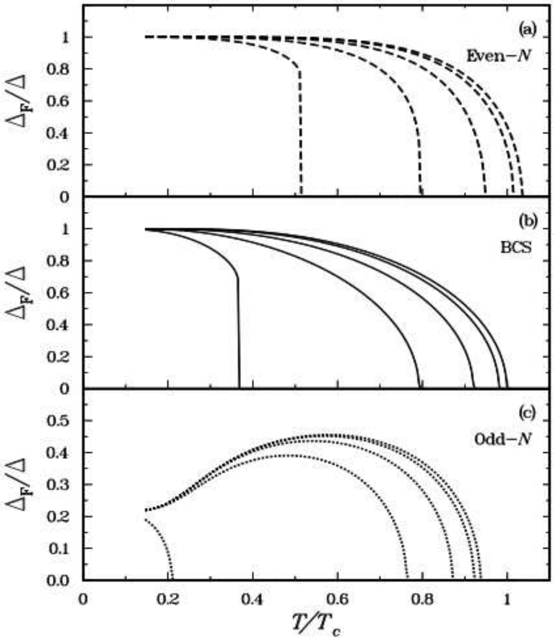

FIG. 2. Dependence upon T of the gap Δ_F for $w_F\Delta = 1.19$ ($w_F\tilde{G} = 0.233$) and for magnetic-field values such that $w_F B$=0; 0.2; 0.4; 0.6; 0.8. The three plots correspond to (a) the even-N projection ($\langle\hat{N}\rangle = 100$), (b) the BCS theory ($\langle\hat{N}\rangle = 100$), and (c) the odd-$N$ projection ($\langle\hat{N}\rangle = 101$). Note the scale difference between (c) and (a).

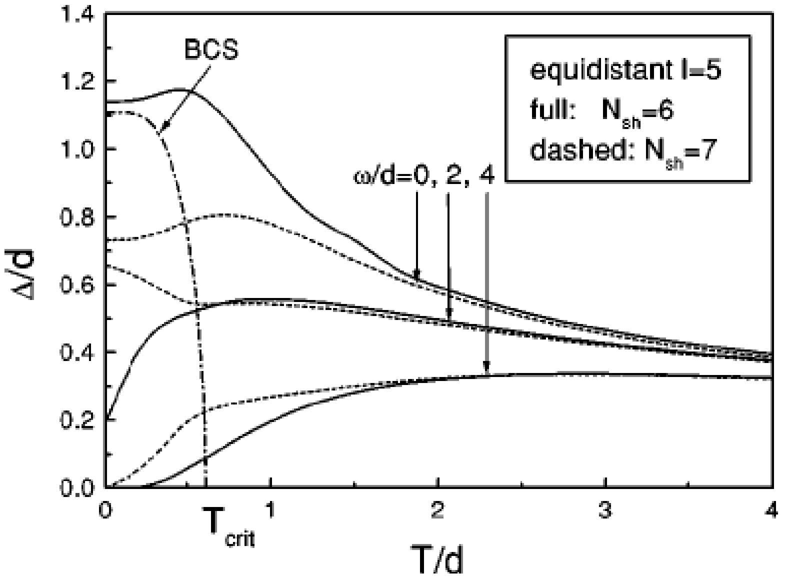

FIG. 5. Canonical gap $\Delta_{can}(T,\omega)$ for an equidistantly spaced l $=5$ shell in a cluster with even (full line) and odd (dotted line) particle number. The mean-field gap $\Delta_{mf}(T,\omega=0)$ is shown by the dash-dotted line (BCS).

- BCS: R. Balian, H. Flocard, and M. Veneroni, Phys. Rep. 317, 251 (1999)
- Seniority Hamiltonian: S. Frauendorf et al., Phys. Rev. B 68, 024518 (2003); J.A. Sheikh, R. Palit, and S. Frauendorf, Phys. Rev. C 72, 041301 (2005)

With increasing temperature, less-aligned excited configurations with lower seniorities enter the canonical ensemble, and this reintroduces the pair correlations. At still higher temperatures, the Meissner transition takes place and pairing correlations decrease.

Fission barriers of compound superheavy nuclei

J. Pei, J. Sheikh, WN, A. Kerman, Phys. Rev. Lett 102, 192501 (2009)
J. Sheikh, WN, J. Pei, Phys. Rev. C 80, 011302(R) (2009)

Unique HFB solvers made this work possible:

HFBAX: J.C. Pei et al., Phys. Rev. C 78, 064306 (2008)
HFODD: J. Dobaczewski and P. Olbratowski, Comput. Phys. Commun. 158, 158 (2004); ibid.167, 214 (2005)

Jądra Superciężkie

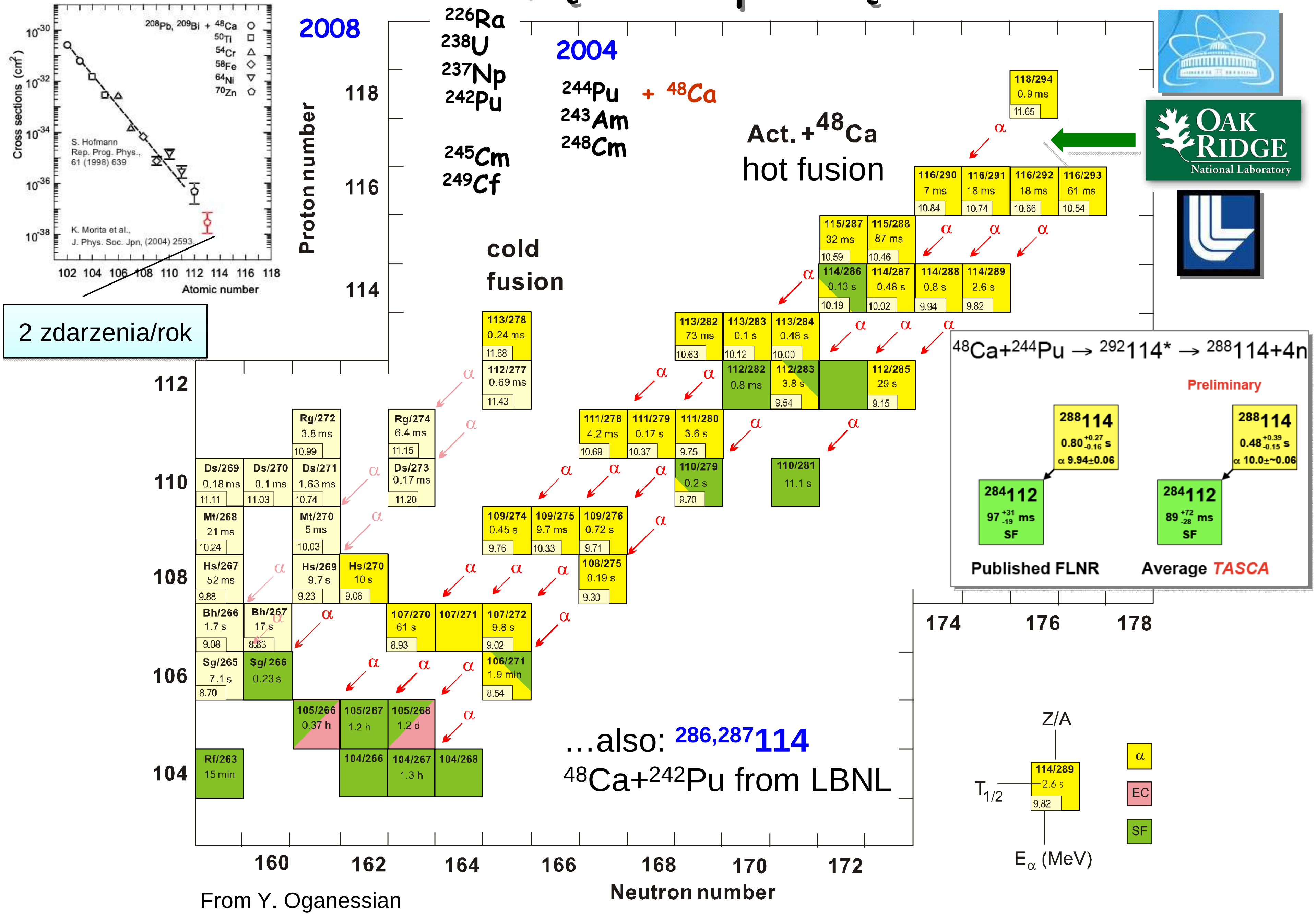

2008

^{226}Ra
^{238}U
^{237}Np
^{242}Pu

^{245}Cm
^{249}Cf

2004

^{244}Pu + ^{48}Ca
^{243}Am
^{248}Cm

Act. + ^{48}Ca
hot fusion

cold
fusion

2 zdarzenia/rok

^{48}Ca+^{244}Pu → ^{292}114* → ^{288}114+4n

Preliminary

Published FLNR	Average *TASCA*
^{288}114 $0.80^{+0.27}_{-0.16}$ s α 9.94±0.06	^{288}114 $0.48^{+0.39}_{-0.15}$ s α 10.0±~0.06
^{284}112 97^{+31}_{-19} ms SF	^{284}112 89^{+72}_{-28} ms SF

…also: ^{286,287}114
^{48}Ca+^{242}Pu from LBNL

From Y. Oganessian

Experiments

- Cold-fusion experiment at GSI **E*=10~12 MeV**
  $(^{70}Zn + ^{208}Pb)\ ^{278}112 \rightarrow ^{277}112 + n$
  S. Hofmann and G. Munzenberg, Rev. Mod. Phys. **72**, *733(2000)*
- Hot-fusion experiment at Dubna **E*=35~40 MeV**
  $(^{48}Ca + ^{244}Pu)\ ^{292}114 \rightarrow ^{288}114 + 4n$
  Y. Oganessian, Pure Appl. Chem. **78**, *889(2006)*
- Highly excited experiment at GANIL **E*~80 MeV**
  $^{208}Pb + Ge, \quad ^{238}U + Ni, \quad ^{238}U + Ge$
  with lifetimes $> 10^{-18}$s for Z=120, 124 and much shorter lifetimes for neutron-deficient nuclei with Z=114
  M. Morjean, et al., Phys. Rev. Lett. **101**, *072701(2008)*

Survival probability of CN is one of the Key issues!

Cold fusion cross sections and fusion probability

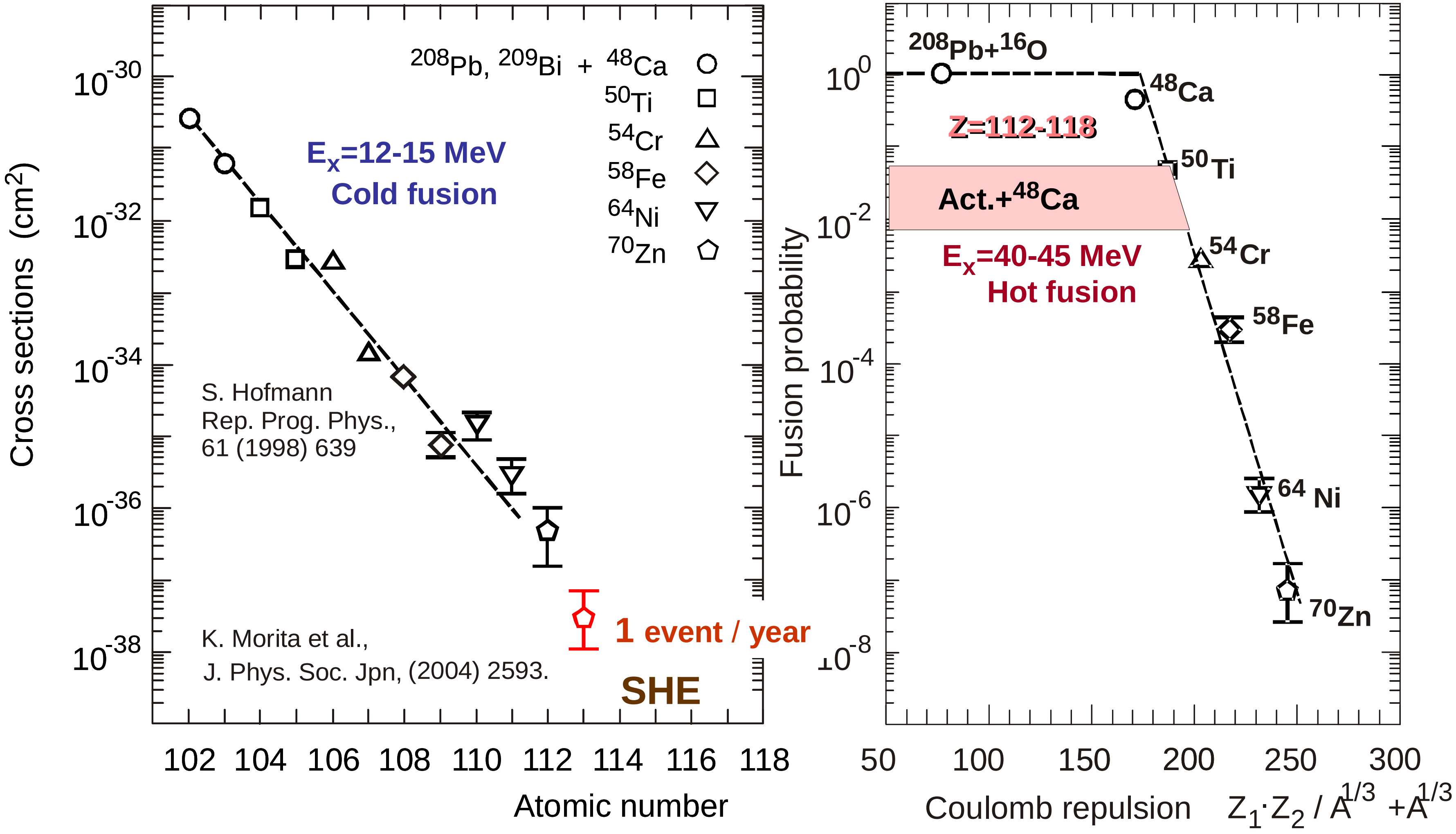

Oganessian, ENAM’08

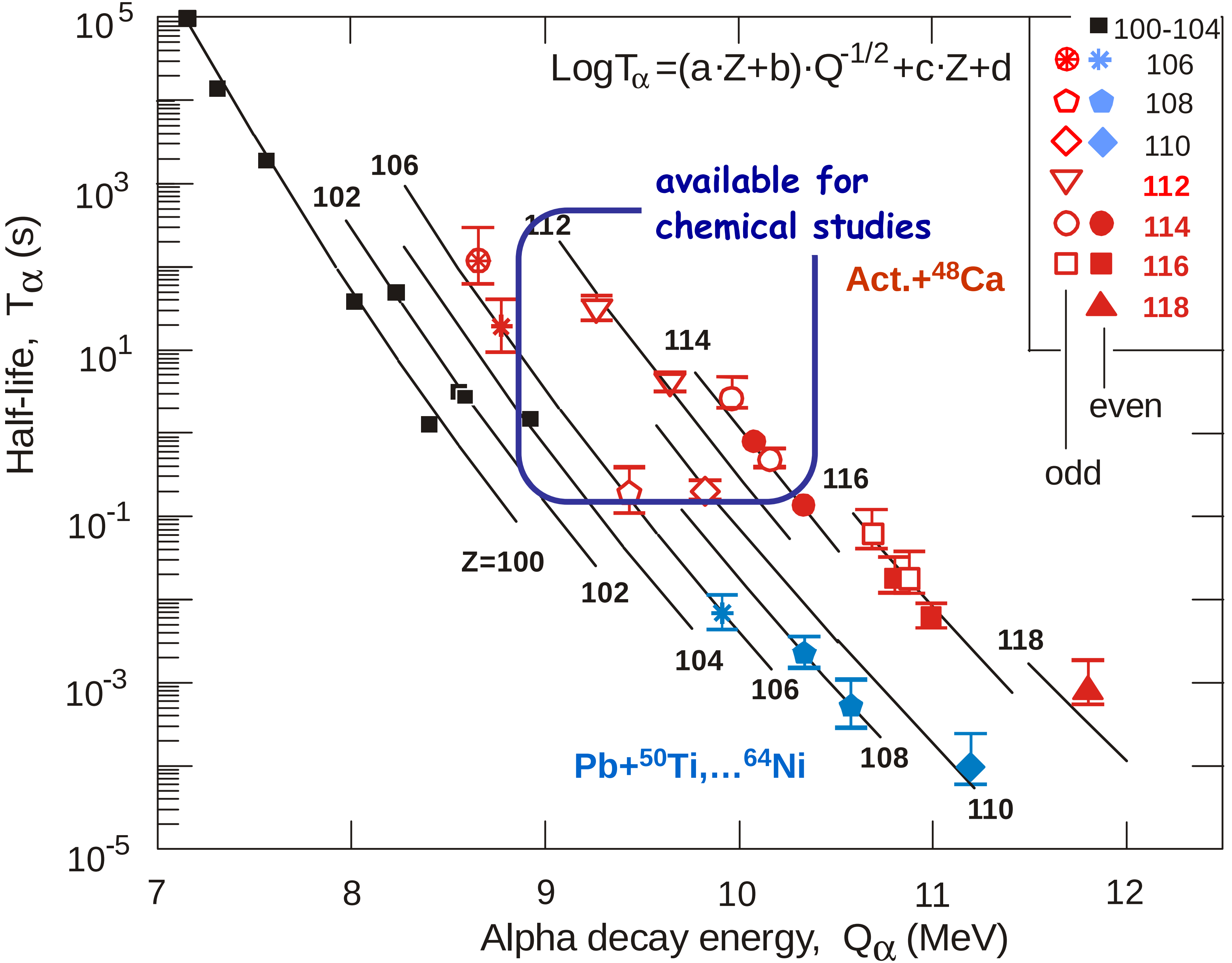

Yu. Oganessian. HE-research at FLNR. ENAM'08, Sept.7-13, 2008, Ryn, Poland

Mean-field Theory at Finite Temperature

- Equilibrium state of a physical system at constant temperature, T and chemical potential, μ is obtained from the minimization of the grand canonical potential

$$\Omega = E - TS - \mu N$$

$$E = \mathrm{Tr}(\hat{D}\hat{H}) \quad , S = -k\mathrm{Tr}(\hat{D}\mathrm{In}\hat{D}) \quad , N = \mathrm{Tr}(\hat{D}\hat{N})$$

- Density operator and the grand partition function are defined as

$$\begin{aligned} \hat{D} &= e^{-\beta(\hat{H}-\mu\hat{N})}/Z \\ Z &= \mathrm{Tr}(e^{-\beta(\hat{H}-\mu\hat{N})}) \end{aligned}$$

- Variation of the grand canonical potential using one-body density operator leads to the following HFB equations

$$\mathcal{H}\begin{pmatrix} U_i \\ V_i \end{pmatrix} = E_i \begin{pmatrix} U_i \\ V_i \end{pmatrix}$$

$$\mathcal{H} = \begin{pmatrix} h-\lambda & \Delta \\ -\Delta^* & -h^* + \lambda \end{pmatrix}$$

- Finite temperature generalizations of the particle and pairing density density matrices are given by

$$\begin{aligned} \rho &= UfU^\dagger + V^*(1-f)\tilde{V} \\ \kappa &= UfV^\dagger + V^*(1-f)\tilde{U} \end{aligned}$$

where the quantity “f” stands for the Fermi function, defined as,

$$f_i = \frac{1}{1+e^{\beta E_i}}$$

Fission: isothermal or isentropic, or …?

M. Diebel, K. Albrecht, and R.W. Hasse, Nucl. Phys. A 355, 66 (1981)
M.E. Faber, M. Ploszajczak, and K. Junker, Acta Phys. Pol. B 15, 94 (1984)

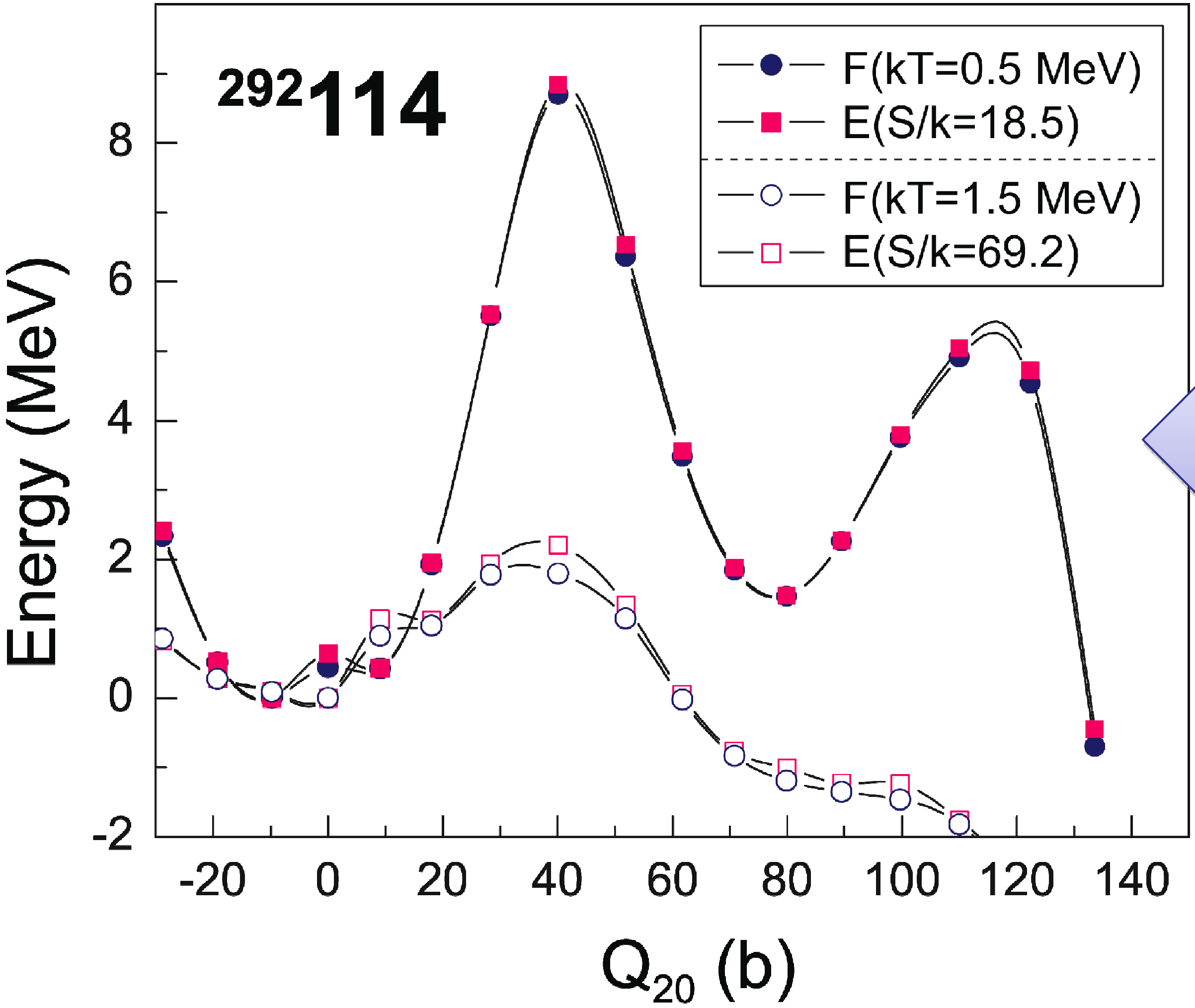

$$\left(\frac{\partial E}{\partial Q_{20}}\right)_S = \left(\frac{\partial F}{\partial Q_{20}}\right)_T$$

Numerical test

The lowest minimum warmer than the saddle point!

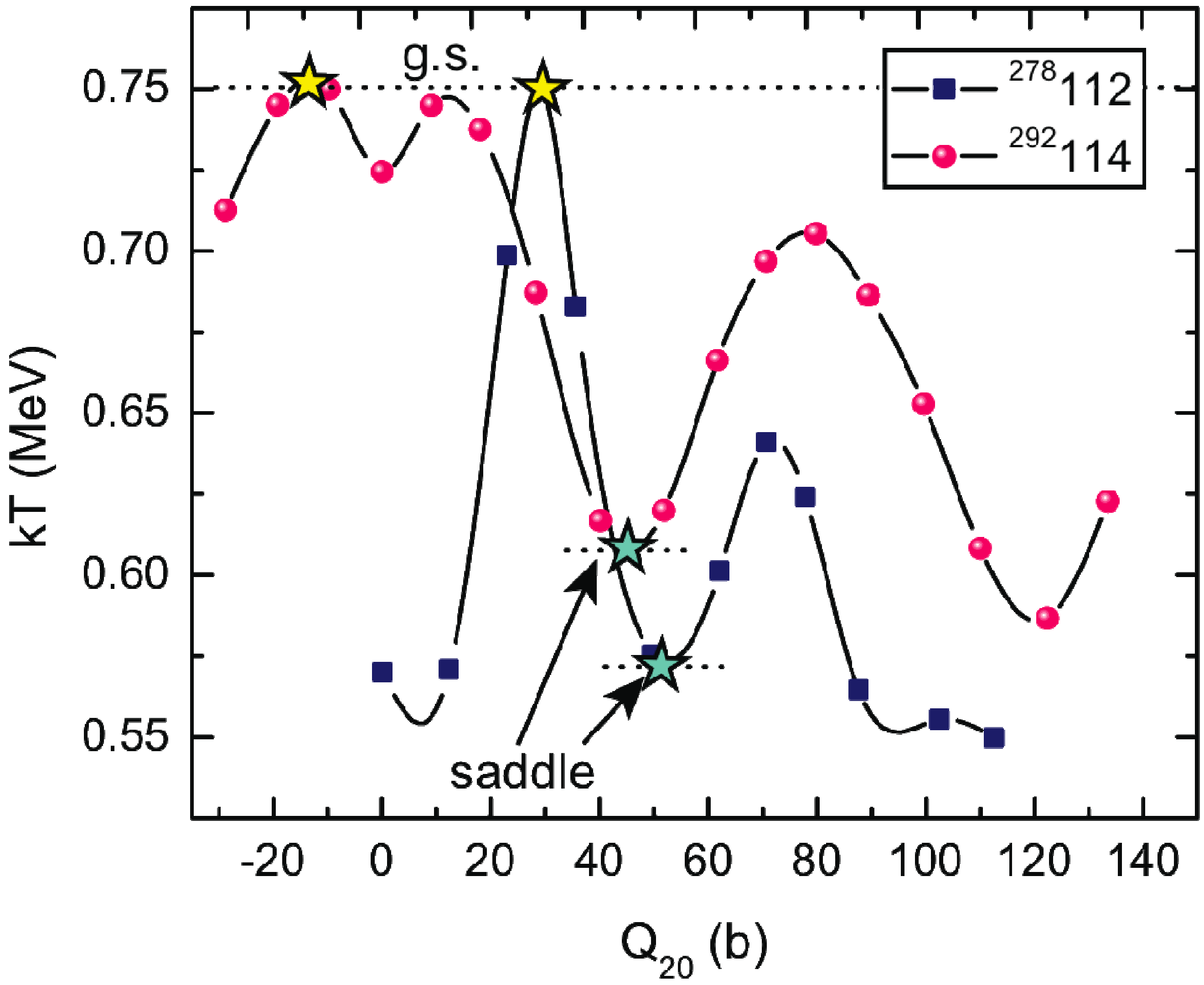

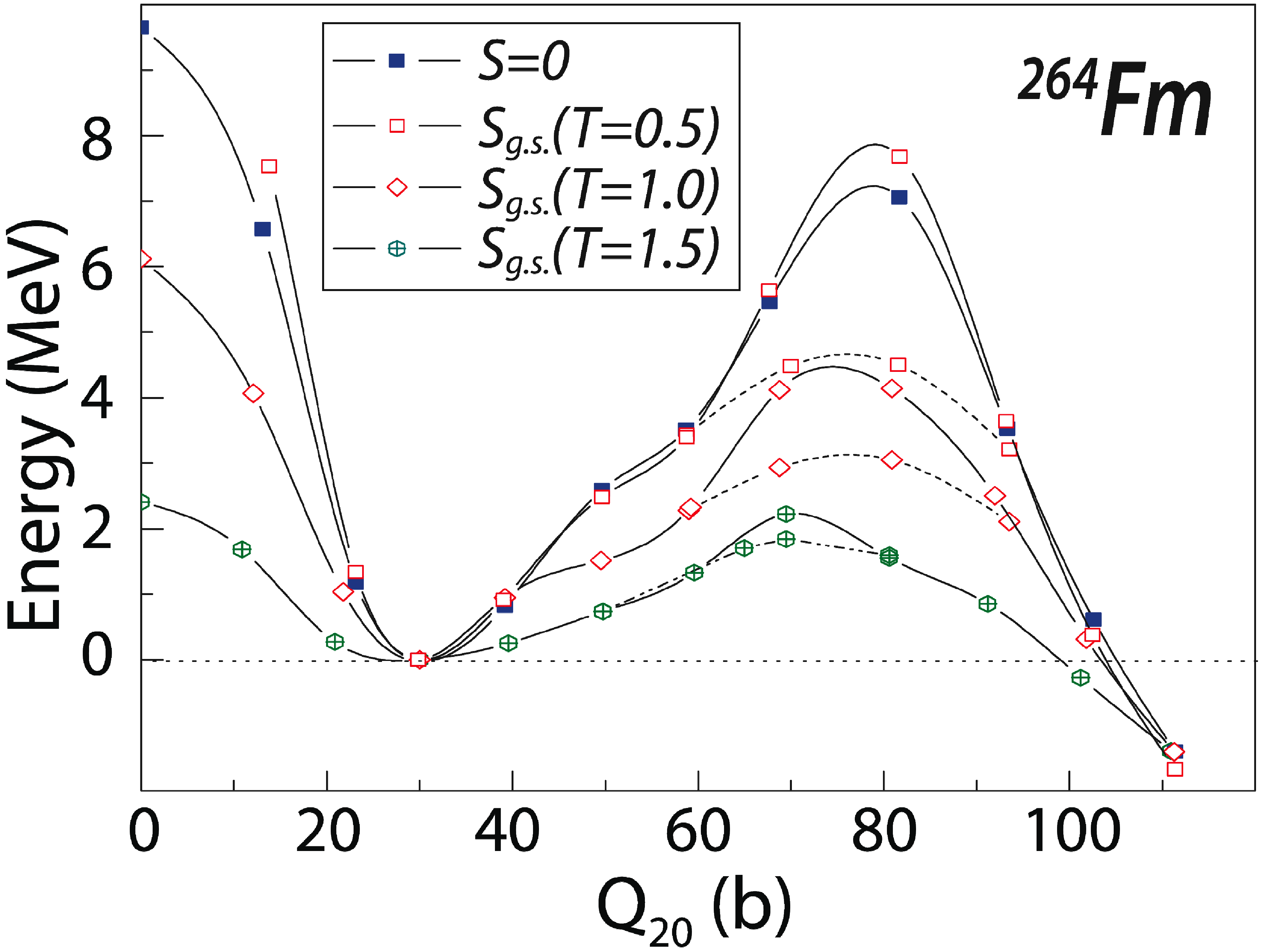
S=0
$S_{g.s.}(T=0.5)$
$S_{g.s.}(T=1.0)$
$S_{g.s.}(T=1.5)$
^{264}Fm
Energy (MeV)
0
2
4
6
8
0
20
40
60
80
100
Q_{20} (b)

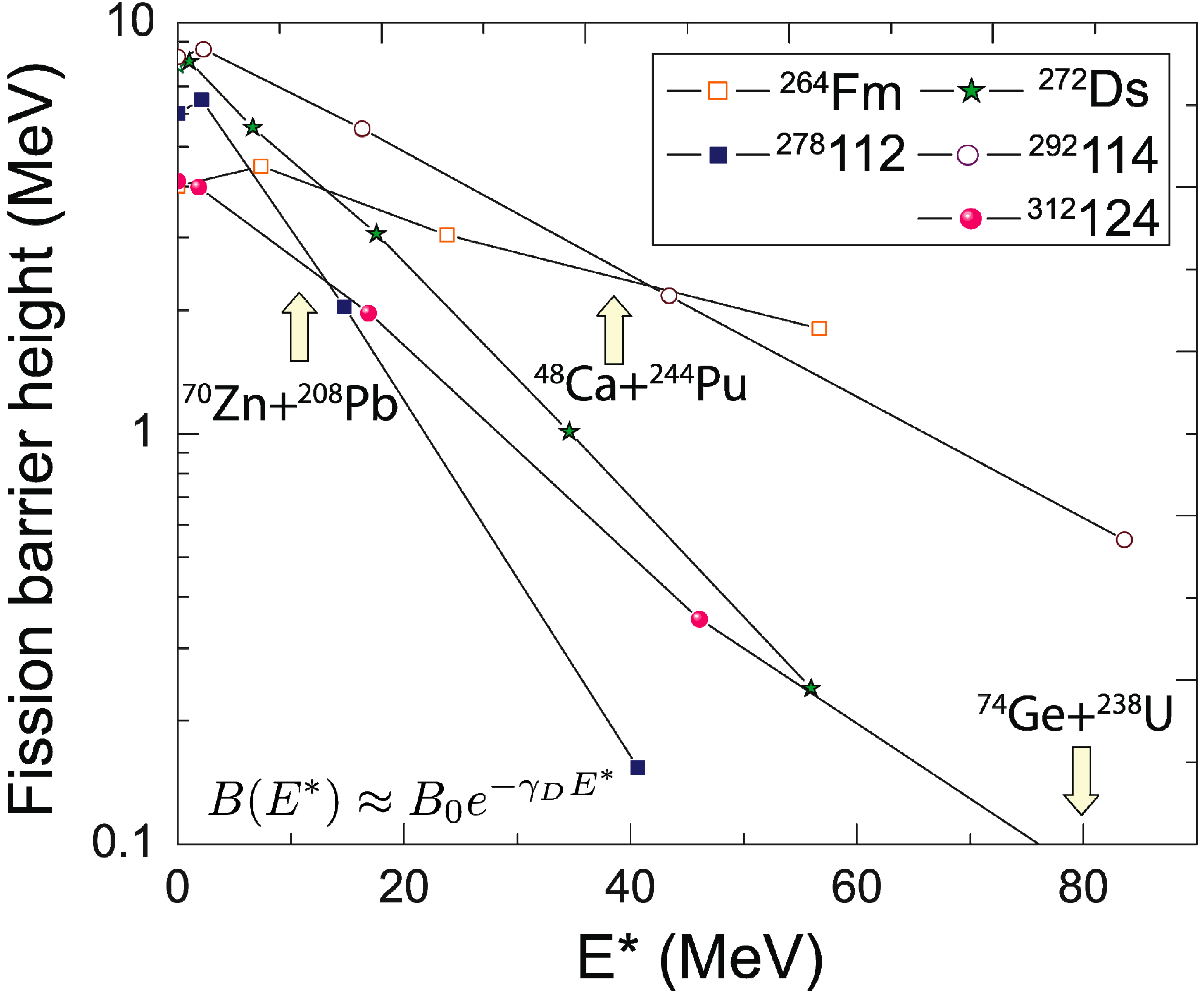
Fission barrier height (MeV)
E* (MeV)
10
1
0.1
0
20
40
60
80
^{264}Fm
^{272}Ds
^{278}112
^{292}114
^{312}124
^{70}Zn+^{208}Pb
^{48}Ca+^{244}Pu
^{74}Ge+^{238}U
$B(E^*) \approx B_0 e^{-\gamma_D E^*}$

$$\Delta T = T_{g.s.} - T_B > 0$$

$$\left(\frac{\partial E}{\partial S}\right)_{Q_{20}} = kT$$

$$\Delta T(^{278}112) > \Delta T(^{292}114)$$

➡ **Shell effects crucial!**

Particle gas component

Can be removed

Its magnitude is related to particle width

P. Bonche, S. Levit, and D. Vautherin, Nucl. Phys. A 427, 278 (1984); 436, 265 (1985)

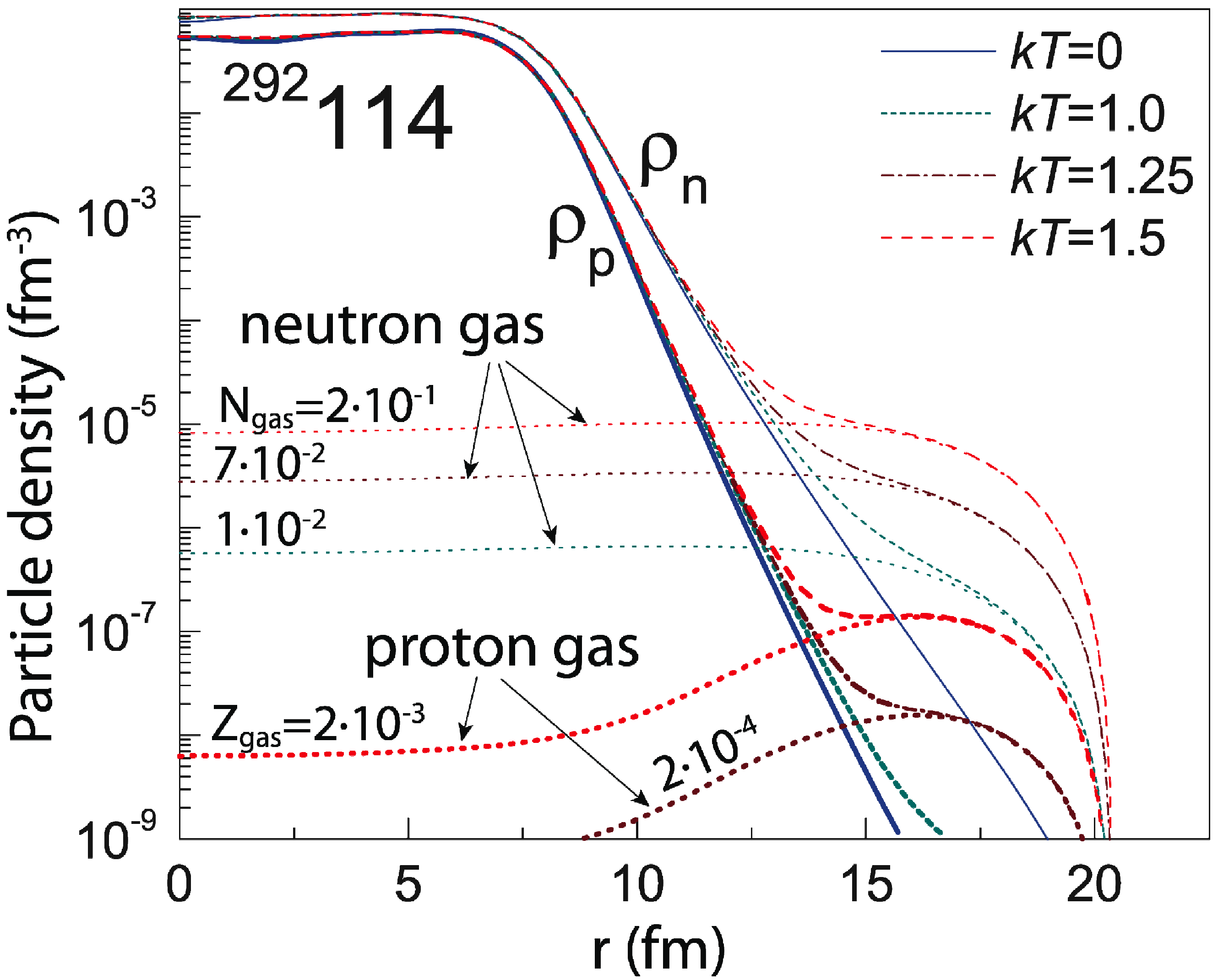

Systematic Study of Fission Barriers of Excited Superheavy Nuclei

J. Sheikh, WN, J. Pei, Phys. Rev. C 80, 011302(R) (2009)

Focus on:

- Mirror asymmetry and triaxiality at high temperatures
- Systematic analysis of barrier damping

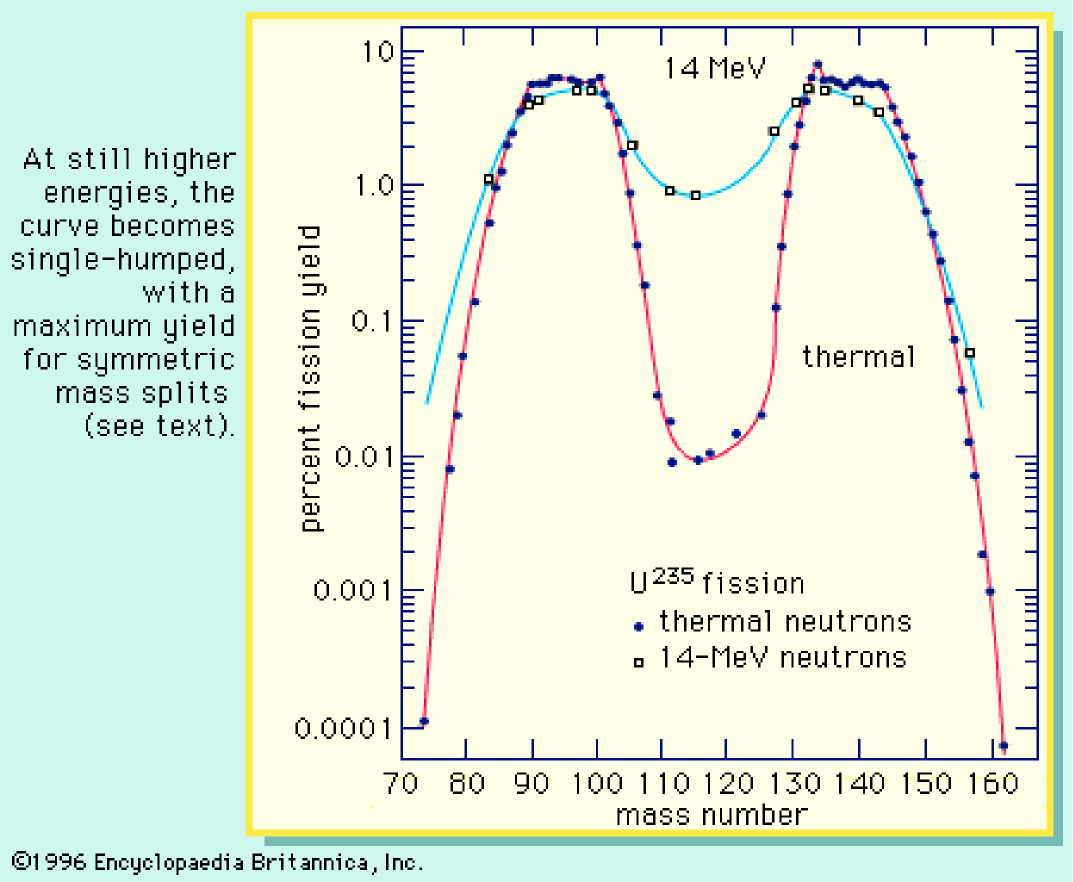

At still higher energies, the curve becomes single-humped, with a maximum yield for symmetric mass splits (see text).

©1996 Encyclopaedia Britannica, Inc.

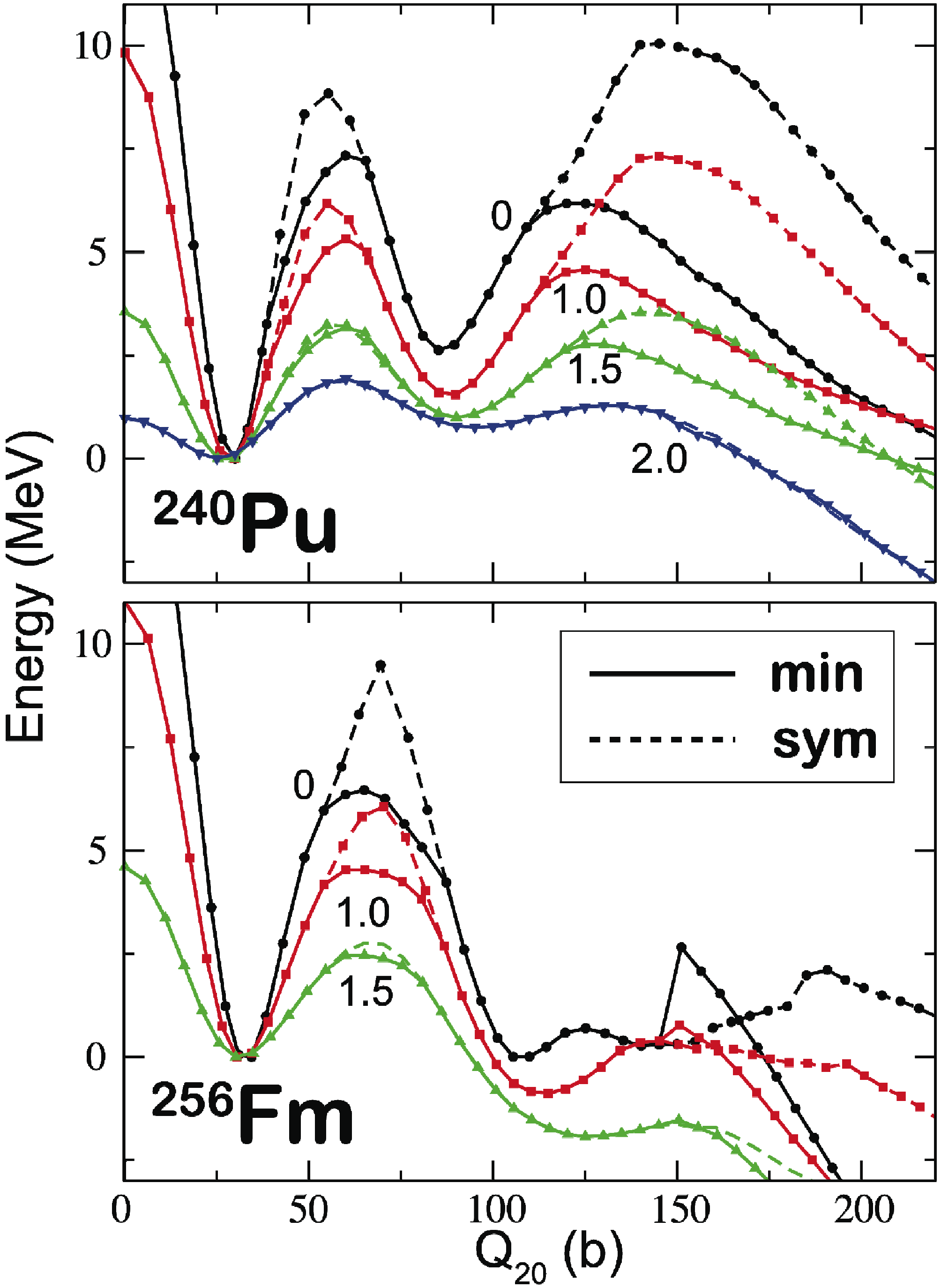

Transition to symmetric split at high-T

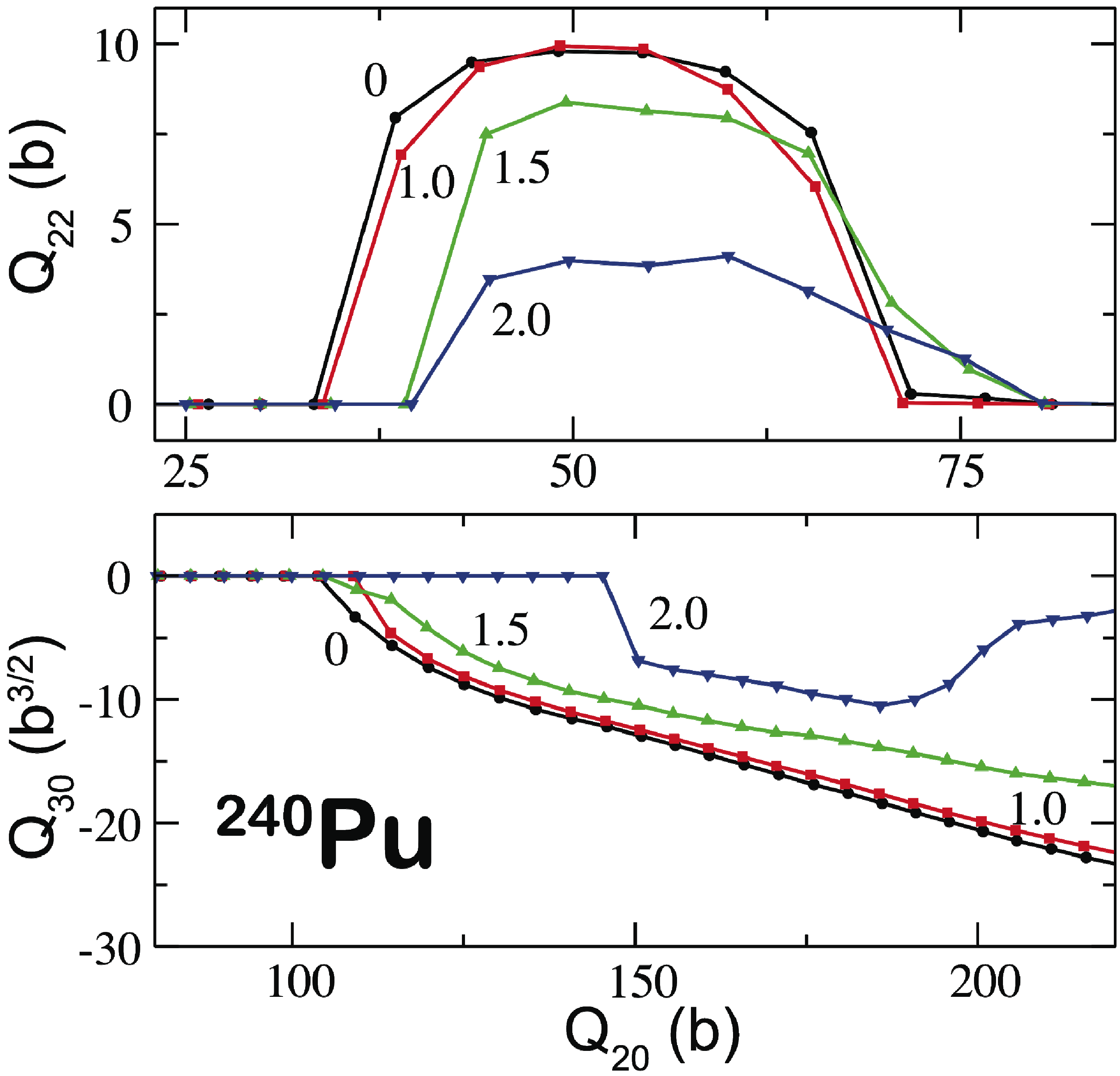
Q_22 (b)
10
5
0
25
50
75
0
1.0
1.5
2.0
Q_30 (b^3/2)
0
-10
-20
-30
100
150
200
Q_20 (b)
240Pu
0
1.5
2.0
1.0

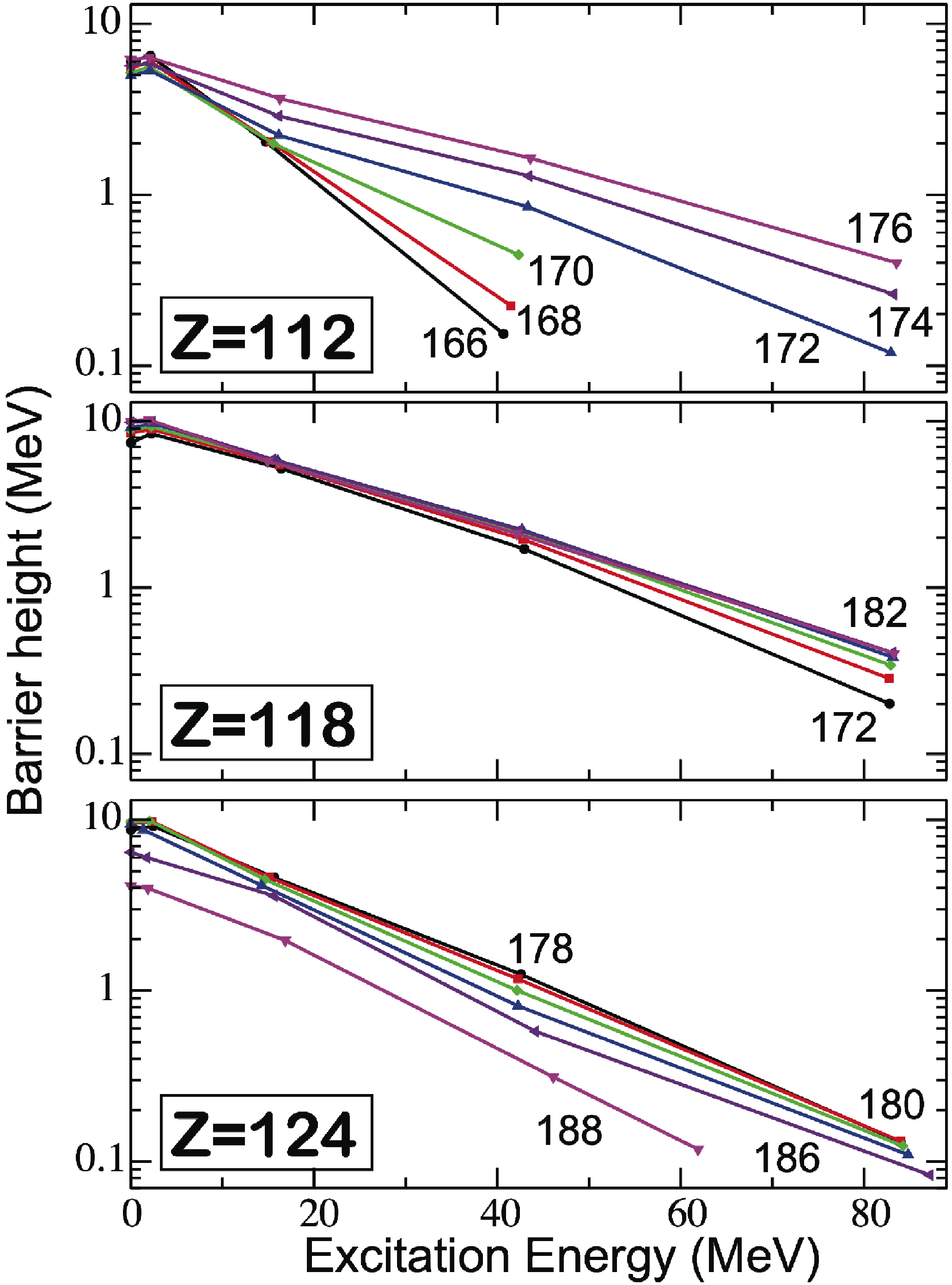

$$B(E^*) = B_0 e^{-\gamma_D E^*}$$

The damping factor can be meaningfully extracted

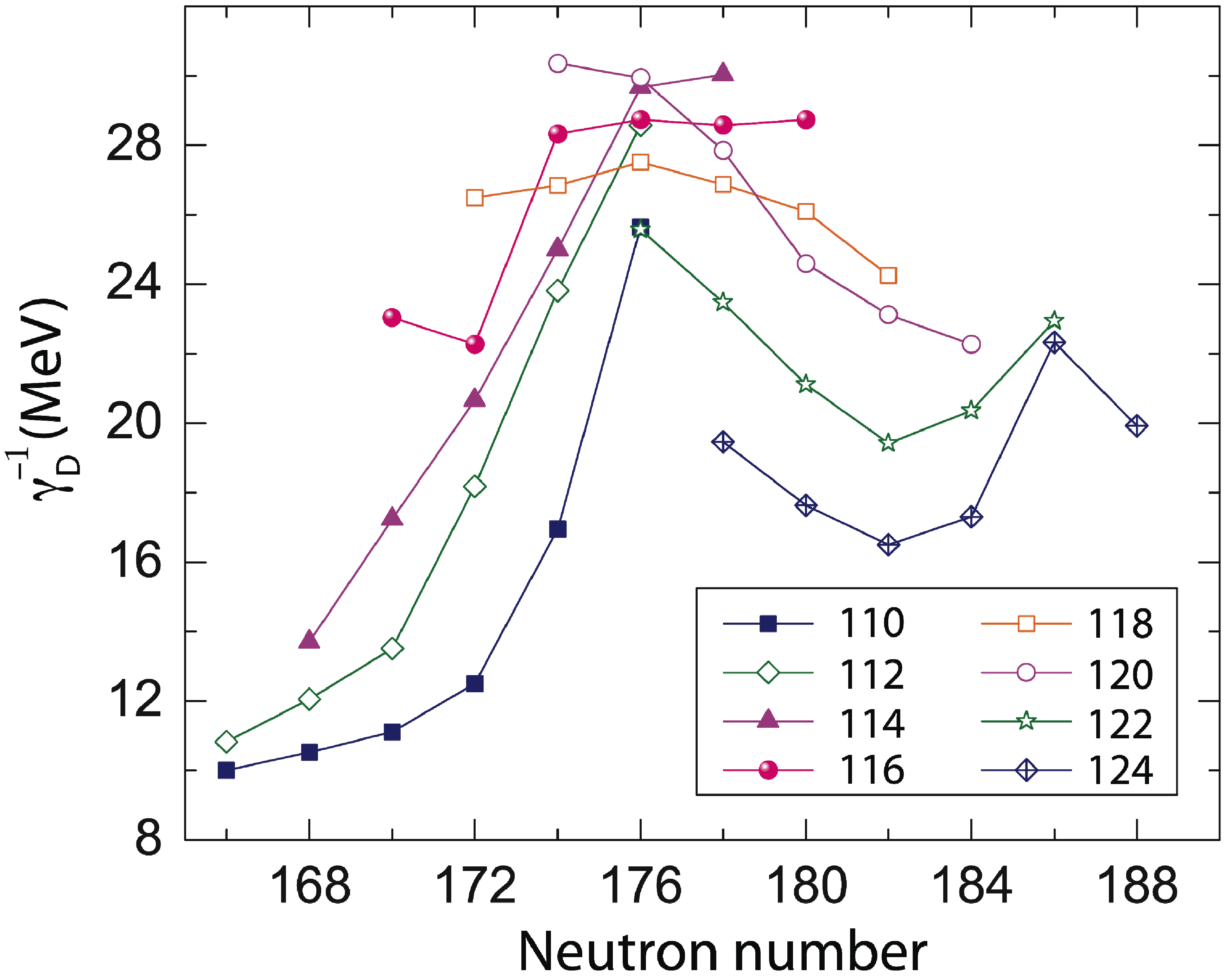
γ_D^{-1} (MeV)
8
12
16
20
24
28
168
172
176
180
184
188
Neutron number
110
112
114
116
118
120
122
124

Microscopic description of spontaneous fission

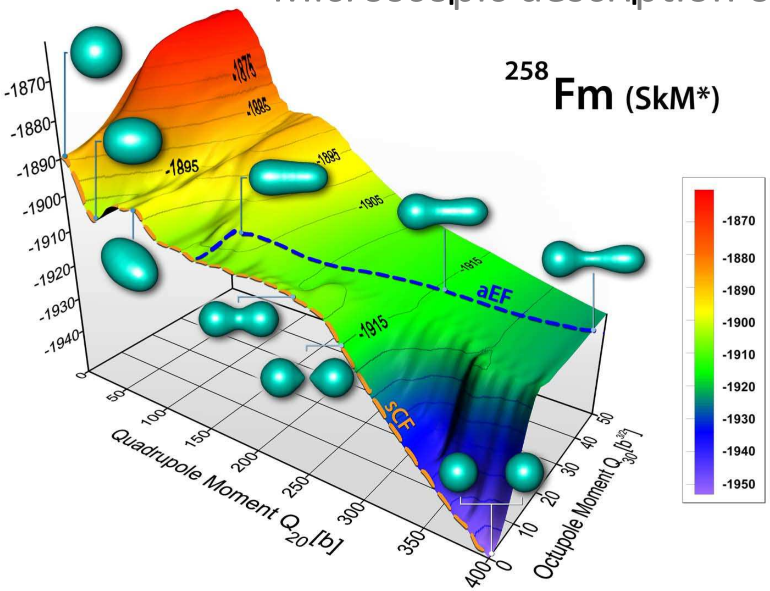

Two-dimensional total energy surface for ^{258}Fm in the plane of two collective coordinates: elongation, Q_{20}, and reflection-asymmetry, Q_{30}. Dashed lines show the fission pathways: symmetric compact fragments (sCFs) and asymmetric elongated fragments (aEFs). Nuclear shapes are shown as three-dimensional images that correspond to calculated nucleon densities.

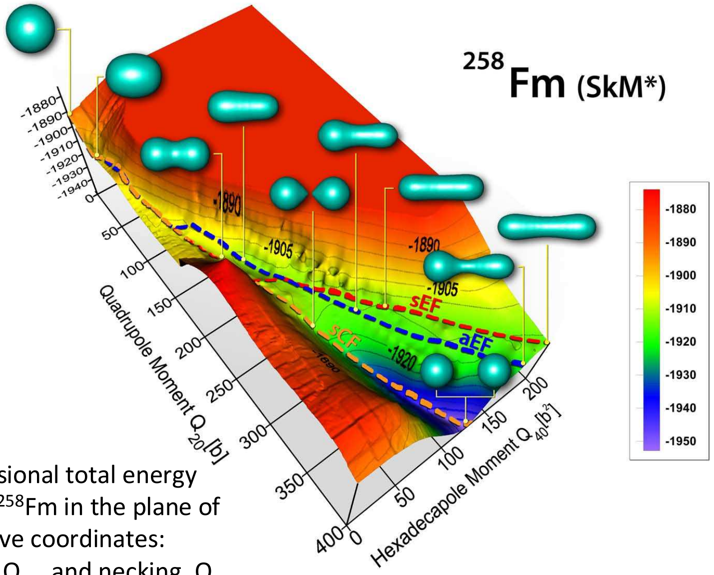

Two-dimensional total energy surface for ^{258}Fm in the plane of two collective coordinates: elongation, Q_{20}, and necking, Q_{40}.

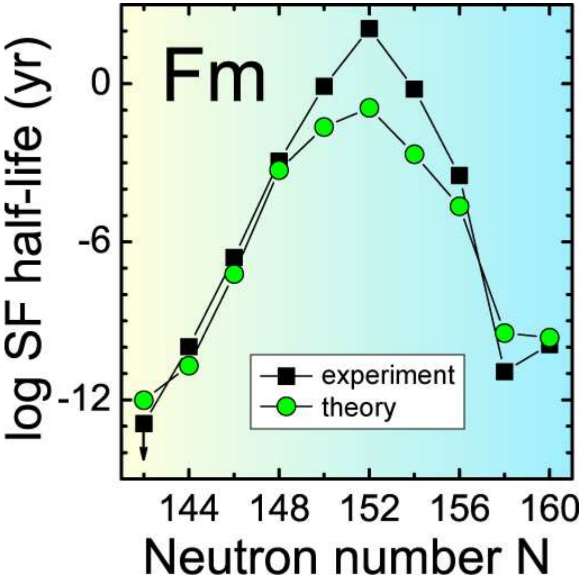

Calculated fission half lives of even-even fermium isotopes, with 242 ≤ A ≤ 260, compared with experimental data.

Summary of fission pathway results obtained in this study. Nuclei around ^{252}Cf are predicted to fission along the asymmetric path aEF; those around ^{262}No along the symmetric pathway sCF. These two regions are separated by the bimodal symmetric fission (sCF + sEF) around ^{258}Fm. In a number of the Rf, Sg, and Hs nuclei, all three fission modes are likely (aEF + sCF + sEF; trimodal fission). In some cases, labeled by two-tone shading with one tone dominant, calculations predict coexistence of two decay scenarios with a preference for one. Typical nuclear shapes corresponding to the calculated nucleon densities are marked.

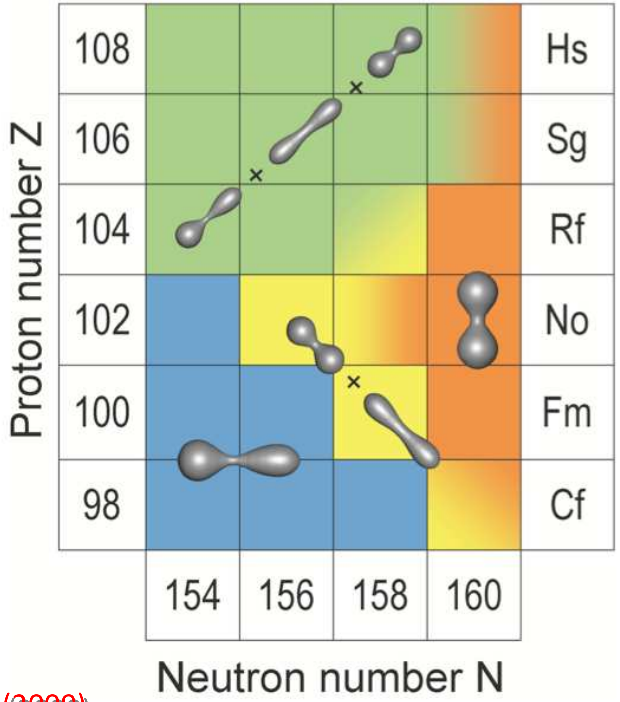

A. Staszczak et al. Phys. Rev. C 80, 014309 (2009)

SciDAC Review, submitted

Microscopic description of spontaneous fission: leadership-class computers help cracking the nuclear puzzle

Advanced theoretical methods and high-performance computers may finally unlock the secrets of nuclear fission, a fundamental nuclear decay that is of great relevance to society.

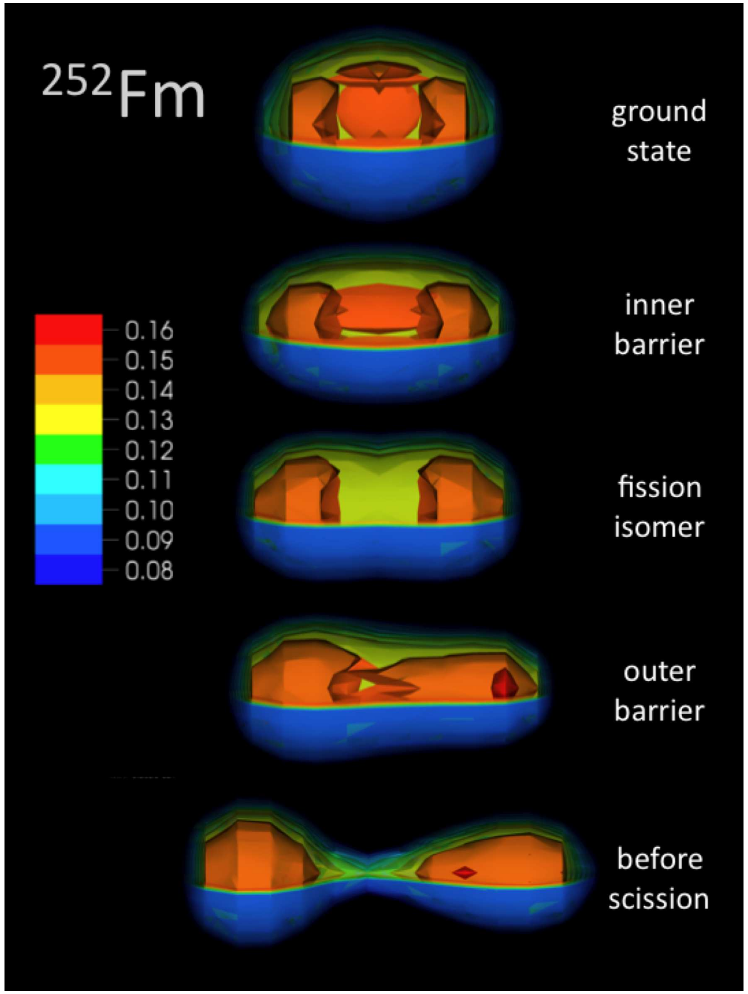

SUMMARY

Two aspects of nuclear behavior at T>0

- Reentrant superconductivity at high spins
- Isentropic fission barriers and shell structure

The role of finite-size effects on pairing in spin-polarized nuclei

Impact of shell effects on survival probability of superheavy compound nuclei

Thank You